Submitted to
32nd International Conference on High Energy Physics, ICHEP04, August 16, 2004, Beijing
Abstract: **12-0766**
Parallel Session **12**
www-h1.desy.de/h1/www/publications/conf/conf_list.html

Search for Lepton Flavor Violation in e^+p Collisions at HERA

H1 Collaboration

Abstract

A search for lepton flavor violating (LFV) processes mediated by leptoquarks (LQ) is performed with the H1 experiment at HERA. Final states with a muon or a tau and a hadronic jet are searched for in a data sample collected in the period 1999-2000 corresponding to an integrated luminosity of $66\ \mathrm{pb}^{-1}$. No evidence for LFV is found. Limits are derived on the Yukawa coupling of LQs to a muon or tau and a light quark, $\lambda_{\mu q,\tau q}$, in the Buchmüller-Rückl-Wyler effective model, as well as on the branching ratio, $BR_{\mathrm{LQ}\to\mu q,\tau q}$, for the LQ decaying to a muon or tau and a light quark.

1 Introduction

In the Standard Model, all known interactions involving leptons conserve the lepton flavors individually. However, from a theoretical point of view, there is no underlying gauge symmetry supporting this experimental observation. In fact, experimental evidence for lepton flavor violation (LFV) in atmospheric neutrino oscillations has already been reported in 1998 [1].

In e^+p collisions at HERA, a LFV process can induce the appearence of a muon or tau instead of the positron in the final state. A convenient concept to explain such exotic signatures is the exchange of a *leptoquark* (LQ). Leptoquarks couple to both quarks and leptons and can therefore be resonantly produced in e^+p collisions at HERA. With this analysis we present a search for LFV processes, where the exchange of a leptoquark leads to a muon or tau in the final state.

2 Phenomenology and Model

Leptoquarks are color triplet scalar or vector bosons, carrying both lepton (L) and baryon (B) number. The fermion number $F = L + 3\,B$ is conserved and takes values of $F = 2$ for e^-q and $F = 0$ for e^+q states. In this analysis, the search for leptoquarks is preformed in e^+p collisions and therefore only leptoquarks with $F = 0$ are considered. Figure 1 illustrates the exotic leptoquark subprocesses in e^+p collisions compared to the hard subprocess in neutral current deep-inelastic scattering (NC DIS). An overview of the Buchmüller-Rückl-Wyler (BRW) effective model [2] using the Aachen notation [3] for the leptoquark coupling to u and d quarks is given in table 1.

For the determination of the signal detection efficiencies the LEGO [4] event generator is used and the complete H1 detector response is simulated. The contributions from several SM background processes which may mimic the signal through measurement fluctuations are evaluated in this analysis. These processes include NC DIS, lepton pair production, W-production, photoprodution and charged current deep-inelastic scattering (CC DIS) modelled by the generators descibed in [5, 6, 7, 8, 9].

3 Data Selection and Analysis Method

During the years 1999/2000, data have been collected with the H1 detector at HERA corresponding to an integrated luminosity of $66\ \mathrm{pb}^{-1}$ of e^+p collisions at a center of mass energy $\sqrt{s} = 319\ \mathrm{GeV}$.

A detailed description of the H1-detector can be found in [10]. The recording of the events is mainly based on the Liquid Argon Calorimeter (LAr) with a trigger efficiency close to 100%. Background events not originating from e^+p collisions are rejected by the requirement that the z-position[1] of the primary vertex is reconstructed within $\pm 35\ \mathrm{cm}$ around the nominal interaction

[1] The incoming proton beam defines the z-axis.

vertex. Further reduction of this background is obtained by using a set of topological filters and by requiring a matching between the event time measured by the central drift chambers and the bunch crossing time.

In the following, an isolated track pointing to a compact electromagnetic cluster is related to an electron. A muon candidate is identified by a track measured in the inner tracking system geometrically matching with signals in the muon system. The hadronic final state is reconstructed from the deposits in the LAr calorimeter in combination with tracking information. The hadrons are then combined into jets using a k_T-algorithm [11]. The identification of the tau is performed in the hadronic decay channel. The signature is a narrow hadronic jet.

The DIS Lorentz invariants Q^2, y, x are used to determine the leptoquark mass, M^{LQ}, with

$$M^{LQ} = \sqrt{xs} = \sqrt{\frac{Q^2}{y}} \, .$$

Here, Q^2 denotes the negative squared momentum transfer, y is the inelasticity of the scattering process and x represents the Bjørken scaling variable.

In order to minimise the dependency on the hadronic energy measurement, the reconstruction of Q^2, y, and x is based on the double angle method [12]. For a LQ decaying into a muon and a quark, the angle of the outgoing muon and the angle of the highest transverse momentum (P_T) jet are taken to reconstruct the mass of the LQ. In the case of the LQ decaying into a high P_T tau and a quark, the angle of the tau is associated with the visible τ-jet and used together with the hadronic jet to reconstruct the kinematics.

3.1 High P_T Muon Signatures

LQs with couplings to second generation leptons, leading to $\mu + q$ final states, show a clear signature in the detector, i.e. an isolated high P_T muon "back-to-back" in the azimuthal angle, ϕ, and balanced in P_T with the hadronic final state. In general, a muon deposits only a very small fraction of its energy in the LAr calorimeter, so the signal is expected to exhibit large P_T^{Calo}, where P_T^{Calo} is the measured P_T reconstructed from all clusters recorded in the calorimeter.

The selections applied in this analysis in the muon channel to identify the LFV signature are:

- Isolated muon preselection:

  1. At least one muon with transverse momentum $P_T^{\mu} > 10$ GeV is required.
  2. The polar angle, θ^{μ}, of the muon track is restricted to be within 10° to 140°.
  3. The muon is required to be isolated with respect to tracks and jets in the event:
     - The distance of the highest P_T muon track to the nearest vertex fitted track in the $\eta\phi$-plane[2] must be greater than 0.5.

[2]Pseudorapidity $\eta = -\ln[\tan(\frac{\theta}{2})]$

- The distance of the highest P_T muon track to the nearest jet in the $\eta\phi$-plane is required to be greater than 1.0.

4. Events with a ratio V_{ap}/V_P lower than 0.3 are selected to reject most of the photoproduction and neutral current events, where the variables

$$V_p = \sum_i \frac{P_T^X \cdot P_T^i}{P_T^X} \text{ for } P_T^X \cdot P_T^i > 0 \ ,$$
$$V_{ap} = \sum_i \frac{P_T^X \cdot P_T^i}{P_T^X} \text{ for } P_T^X \cdot P_T^i < 0$$

are deduced by summing over all particles in the detector and where P_T^X is the total transverse momentum.

5. Only events with calorimetric transverse momentum (P_T^{Calo}) greater than 12 GeV are selected.

- Subsequent LFV signal selection:

1. Events are required to have no electron in the electromagnetic LAr.
2. Exactly one isolated muon is required.
3. Events are selected with an azimuthal angle between the hadronic final state and the isolated muon (acoplanarity) greater than 170°.
4. P_T^{Calo} is required to be greater than 25 GeV.

Figure 2 shows control distributions of acoplanarity, V_{ap}/V_P, P_T^{Calo} and P_t^μ after applying the isolated muon selection. The selected data is well described by the SM Monte Carlo simulation.

3.2 High P_T Tau Signatures

We restrict the search for leptoquarks possessing couplings to a third generation lepton leading to $\tau + q$ final states to the hadronic decays of the τ. The hadronic decays of a high P_T tau lead to a typical signature of a high P_T "pencil-like" τ-jet. This τ-jet is characterised by a narrow shape in the calorimeter and low track multiplicity, i.e. one to three tracks in the identification cone of the jet. The neutrinos from the decay of the tau are boosted with the hadrons in the direction of the τ-jet. Therefore, the signal topology is a dijet event with no leptons. The missing transverse momentum in the event carried by the neutrino is aligned with the second highest P_T jet (jet2), which has to fulfil the τ-jet criteria.

The following selection criteria are applied:

- Selection of high P_T dijet events with no lepton:

1. There is no $e^\pm$ or $\mu^\pm$ found in the event.
2. There are at least 2 jets in the event with:

  - $P_T^{\mathrm{jet1}} > 25$ GeV
  - $P_T^{\mathrm{jet2}} > 15$ GeV
  - both jets in the angular range $7^\circ < \theta^{\mathrm{jet}} < 145^\circ$
  - electromagnetic fraction of both jets: $f_{em}^{\mathrm{jet}} < 0.95$

- Selection of events with jet2 fulfilling τ-jet criteria:

  1. Large missing transverse momentum: $P_T^{\mathrm{miss}} > 20$ GeV.
  2. Number of tracks in identification cone of jet2: $1 \leq N_{\mathrm{tracks}}^{\mathrm{jet2}} \leq 3$.
  3. No tracks in an outer cone in the $\eta\phi$-plane around jet2 with $0.12 < D_{track} < 1.0$.
  4. Mass of jet2: $M^{\mathrm{jet2}} < 7$ GeV.
  5. Radius of jet2 in $\eta\phi$-plane: $R^{\mathrm{jet2}} < 0.12$.
  6. P_T^{miss} in direction of jet2: $|\phi^{\mathrm{jet2}} - \phi^{\mathrm{miss}}| < 30^\circ$.

Figure 3 shows control distributions for P_T^{miss}, R^{jet2}, D_{track} and M^{jet2}, which are well reproduced by the SM expectation.

3.3 Systematic Uncertainties

Table 2 lists the systematic uncertainties for the MC simulation of the dominant SM background processes. These uncertainties are deduced from the agreement between data and simulation in the control studies.

The experimental uncertainties on the muon energy is 5%. The errors attributed to the polar and azimuthal angle measurement are 3 mrad and 1 mrad respectively. The muon identification uncertainty is 6%. The uncertainty on the hadronic energy scale is 2% and the uncertainty of the polar and azimuthal angles of the hadronic system are 10 mrad each. The uncertainty on the luminosity measurement is 1.5%. The following uncertainties are related to the modelling of the LQ signal and the CTEQ5 parametrisation of the parton density functions [13]:

- The theoretical uncertainty on the signal cross section due to uncertainties in the parton densities varies from 7% for $e^+u \rightarrow \mathrm{LQ}$ at low LQ masses up to 50% at high LQ masses for $e^+d \rightarrow \mathrm{LQ}$.

- Choosing either Q^2 or the square of the transverse momentum of the final state lepton instead of the center of mass energy of the hard subprocess, $\sqrt{sx}$, as the hard scale at which the proton distributions are estimated, yields an uncertainty of 7% on the signal process.

4 Results

The results of the selections in the muon and tau channel are summarized in table 3. The final mass spectra for both selections are shown in figure 4.

No event is selected in the muon channel with an expectation of 0.74 ± 0.25 events from the Standard Model processes. The largest contribution to this SM background comes from muon-pair production. The selection efficiency for LQs decaying to $\mu + q$ is 60% for a vector LQ of mass 100 GeV and rises up to 75% at masses $150 - 200$ GeV. Near the kinematic limit it falls steeply to 33%. This fall due to the high P_T requirements observed for vector LQs in both the muon and tau decay channel can be explained by the behaviour of the signal cross section near the kinematic limit [4]. For a scalar LQ the efficiency is 65% at masses of 100 GeV and reaches 70% at 150 GeV and then falls gradually to 40% above the kinematic limit.

One data event is found as a high P_T tau candidate from a LQ decay compared to a SM expectation of 0.56 ± 0.16. This SM background is dominated by NC DIS and photoproduction. The selection efficiency for the LFV signal of scalar LQs decaying to a $\tau + q$ final state varies between 12% at a LQ mass of 100 GeV and 24% at $200 - 250$ GeV. For vector LQs the efficiency rises up to 32% and falls steeply near the kinematic limit of $\sqrt{s} = 319$ GeV to become stable at 10% above the kinematic limit.

In order to set limits on the signal cross section, the mass spectra are scanned for signals using a sliding mass window with optimised borders. Within this window the number of data events, background events and the selection efficiency are used to calculate an upper limit on the signal at a 95% confidence level (CL) [14]. These limits are converted into limits on the couplings $\lambda_{\mu q}$ and $\lambda_{\tau q}$. The obtained limits are shown in figure 5 for scalar and vector LQs with an assumed LFV branching ratio of $BR_{\mathrm{LQ}\to\mu q,\tau q} = 0.5$.

Figure 6 illustrates the limits on the coupling constants for the scalar LQ $S^L_{1/2}$ and the vector LQ V^L_1 of the present analysis in comparison with previous limits set by the H1 experiment on LQs coupling to first generation leptons only. These previous results are obtained with additional data of luminosity $\mathcal{L} = 37\ \mathrm{pb}^{-1}$ at a centre of mass energy $\sqrt{s} = 301$ GeV [15].

The limit calculation is extended to different branching ratios fixing λ_{eq} at the electromagnetic coupling strength of 0.3. Figure 7 shows limits on $BR_{\mathrm{LQ}\to\mu q,\tau q}$ with the scalar LQ $S^L_{1/2}$ and the vector LQ V^L_1 in both decay channels, $\mathrm{LQ} \to \mu q$ and $\mathrm{LQ} \to \tau q$.

5 Conclusions

A search for LFV mediated by LQs coupling to second and third generation leptons in e^+p collisions has been performed at HERA using a data sample corresponding to an integrated luminosity $\mathcal{L} = 66\ \mathrm{pb}^{-1}$ collected with the H1 detector at a centre of mass energy $\sqrt{s} = 319$ GeV. No evidence has been found for lepton flavor violation in the muon or tau decay channel. Exclusion limits for coupling constants and branching ratios have been set in a LQ mass range of 100 to 400 GeV. Taking a Yukawa coupling constant of electromagnetic strength, couplings of scalar (vector) LQs with masses up to 275-300 (288-330) GeV to second generation leptons and couplings of scalar (vector) LQs with masses up to 260-284 (278-300) GeV to third generation leptons are excluded. A comparison with previous limits on the coupling constant for LQs coupling to first generation leptons show a similar behaviour.

References

[1] Y. Fukuda *et al.* [Super-Kamiokande Collaboration], Phys. Rev. Lett. **81** (1998) 1562 [hep-ex/9807003].

[2] W. Buchmüller, R. Rückl and D. Wyler, Phys. Lett. B **191** (1987) 442.

[3] B. Schrempp, Physics at HERA: Proceedings of the Workshop, eds. W. Buchmüller and G, Ingelmann, Vol. 2, pp.1034-1042, Hamburg, Germany, 1991.

[4] K. Rosenbauer, dissertation RWTH Aachen (in German), PITHA 95/16, July 1995.

[5] H. Jung, Hard diffractive scattering in high-energy ep collisions and the Monte Carlo generation RAPGAP, Comput. Phys. Commun. **86** (1995) 147; RAPGAP program manual (1998) unpublished [http://www-h1.desy.de/∼jung/RAPGAP.html].

[6] T. Abe, GRAPE-Dilepton (Version 1.1): A generator for dilepton production in ep collisions, Comput. Phys. Commun. **136** (2001) 126 [hep-ph/0012029].

[7] U. Baur,J. A .M. Vermaseren and D. Zeppenfeld, H1 generator based on EPVEC 1.0, Nucl. Phys. B **375** (1992) 3.

[8] T. Sjöstrand, PYTHIA 5.7, CERN-TH-6488 (1992), Comp. Phys. Comm. **82** (1994) 74.

[9] G.A. Schuler and H. Spiesberger, DJANGO 2.1, Proc. of the Workshop "Physics at HERA" (1991), Eds. W. Buchmüller and G. Ingelman, Vol. 3, p. 1419.

[10] I. Abt *et al.* [H1 Collaboration], Nucl. Instrum. Meth. A **386** (1997) 310;
I. Abt *et al.* [H1 Collaboration], Nucl. Instrum. Meth. A **386** (1997) 348.

[11] J.M. Butterworth, J.P. Couchman, B.E. Cox, B.M. Waugh, KTJET: A C++ implementation of the k-perpendicular clustering algorithm, Comput. Phys. Commun. **153** (2003) 85 [hep-ph/0210022].

[12] U. Bassler, G. Bernardi, Nucl. Instrum. Meth. A **426** (1999) 583 [hep-ex/9801017].

[13] H.L. Lai *et al.* [CTEQ collaboration], Eur. Phys. J. C **12** (2000) 375 [hep-ph/9903282].

[14] T. Junk, Nucl. Instrum. Meth. A **434** (1999) 435.

[15] C. Adloff *et al.* [H1 Collaboration], A Search for Leptoquark Bosons in ep Collisions at HERA, Int. Europhysics Conf. on High Energy Physics, Jul 17-23, 2003, Aachen, Abstract 105, Parallel Session 13 .

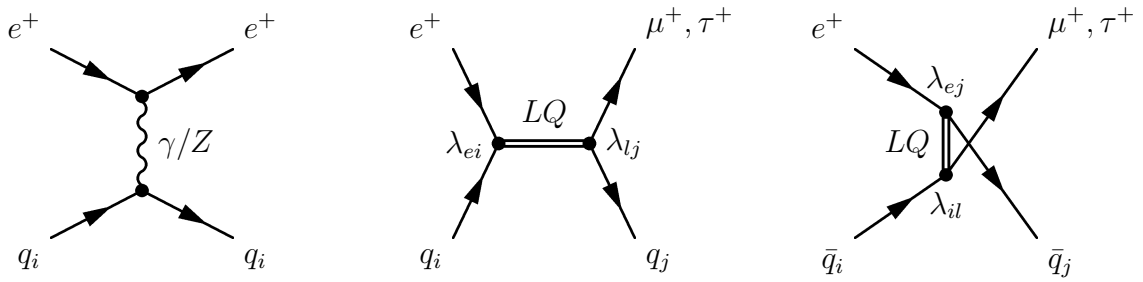

Figure 1: Left: NC deep-inelastic scattering. Centre: s-channel resonant LQ production and decay mediating LFV. Right: u-channel exchange of a LQ possessing couplings to second or third generation leptons.

Q	$F=2$	Prod./Decay	Coupl.	BR	Q	$F=0$	Prod./Decay	Coupl.	BR
Scalar Leptoquarks									
+1/3	S_0^L	$e_L^+\bar{u}_L \to l^+\bar{u}$	λ_L	1/2	+5/3	$S_{1/2}^L$	$e_L^+u_L \to l^+u$	λ_L	1
+1/3	S_0^R	$e_R^+\bar{u}_R \to l^+\bar{u}$	λ_R	1	+5/3	$S_{1/2}^R$	$e_R^+u_R \to l^+u$	λ_R	1
+4/3	$\tilde{S}_0^R$	$e_R^+\bar{d}_R \to l^+\bar{d}$	λ_R	1	+2/3		$e_R^+d_R \to l^+d$	$-\lambda_R$	1
+1/3	S_1^L	$e_L^+\bar{u}_L \to l^+\bar{u}$	$-\lambda_L$	$\frac{1/2\bar{u}+2\bar{d}}{\bar{u}+2\bar{d}}$	+2/3	$\tilde{S}_{1/2}^L$	$e_L^+d_L \to l^+d$	λ_L	1
+4/3		$e_L^+\bar{d}_L \to l^+\bar{d}$	$-\sqrt{2}\lambda_L$						
Vector Leptoquarks									
+4/3	$V_{1/2}^L$	$e_L^+\bar{d}_R \to l^+\bar{d}$	λ_L	1	+2/3	V_0^L	$e_L^+d_R \to l^+d$	λ_L	1/2
+1/3	$V_{1/2}^R$	$e_R^+\bar{u}_L \to l^+\bar{u}$	λ_R	1	+2/3	V_0^R	$e_R^+d_L \to l^+d$	λ_R	1
+4/3		$e_R^+\bar{d}_L \to l^+\bar{d}$	λ_R	1	+5/3	$\tilde{V}_0^R$	$e_R^+u_L \to l^+u$	λ_R	1
+1/3	$\tilde{V}_{1/2}^L$	$e_L^+\bar{u}_R \to l^+\bar{u}$	λ_L	1	+5/3	V_1^L	$e_L^+u_R \to l^+u$	$\sqrt{2}\lambda_L$	$\frac{1/2d+2u}{d+2u}$
					+2/3		$e_L^+d_R \to l^+d$	$-\lambda_L$	

Table 1: Isospin families of leptoquarks in the Buchmüller-Rückl-Wyler model [2] and the decay channels considered in this analysis. The superscript of the leptoquark indicates the chirality of the lepton involved, whereas the subscript corresponds to the weak isospin. Different chiralities between the lepton and the quark lead to vector leptoquarks with Spin $I = 1$ and equal chiralities give scalar leptoquarks with Spin $I = 0$. For left-handed leptoquarks with whole-numbered weak isospin, the branching ratio BR accounts for an additional charged current decay channel, i.e. the decay into a neutrino and a quark.

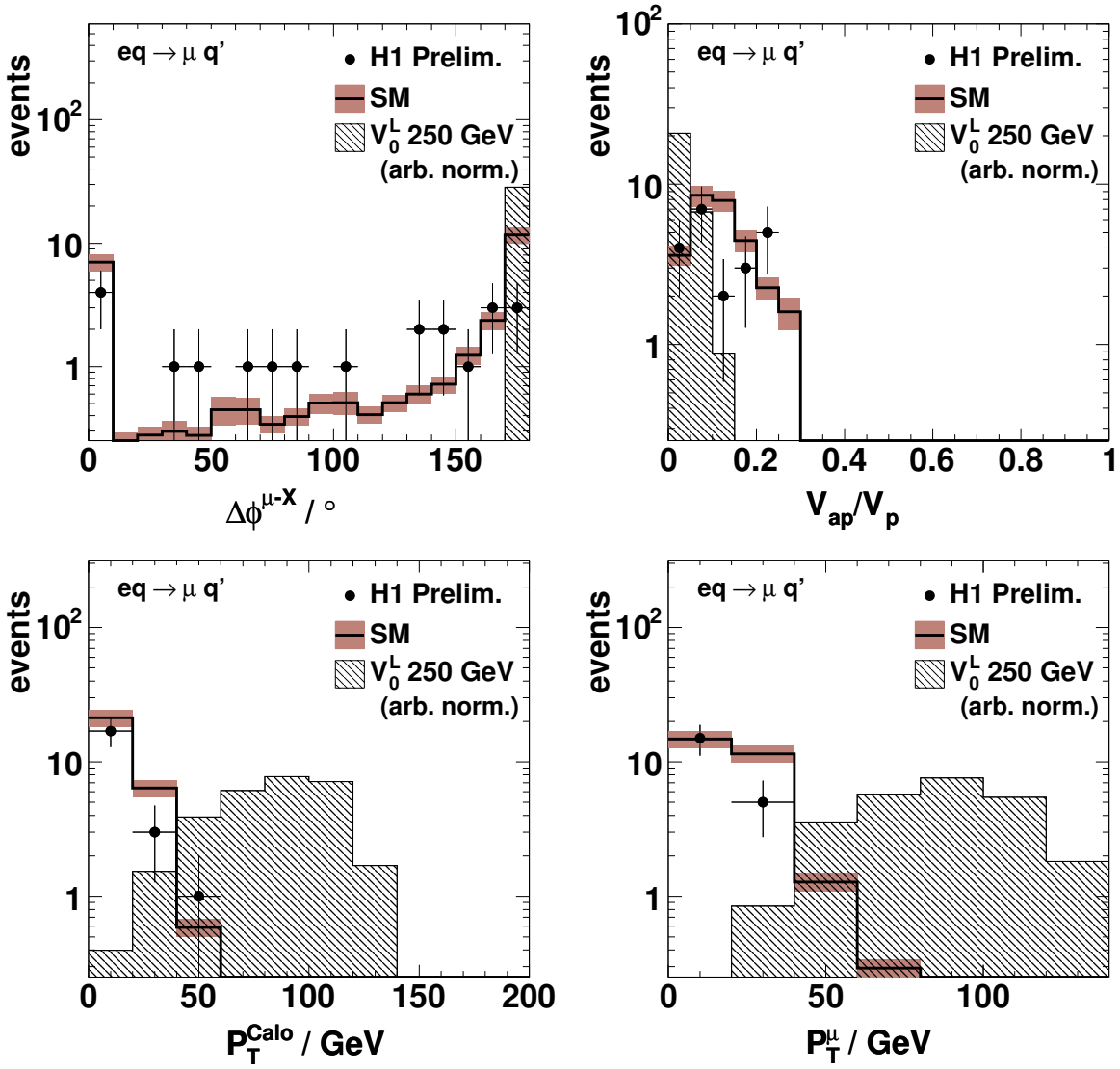

Figure 2: Distributions of H1 data in the muon channel after the isolated muon selection step with SM expectation and arbitrarily normalised LFV signal mediated by a vector LQ, V_0^L, of mass 250 GeV decaying to a muon and a quark. The acoplanarity (top left), shows the clear back-to-back nature of the LQ decay products (hatched histogram) where the azimuthal angle between the hadronic system and the muon is around $180°$. V_{ap}/V_P (top right) shows the lack of isotropy in the selected events. P_T^{Calo} (bottom left) and P_T^{μ} (bottom right) show the transverse momentum sum deposited in the calorimeter and the muon transverse momentum, respectively.

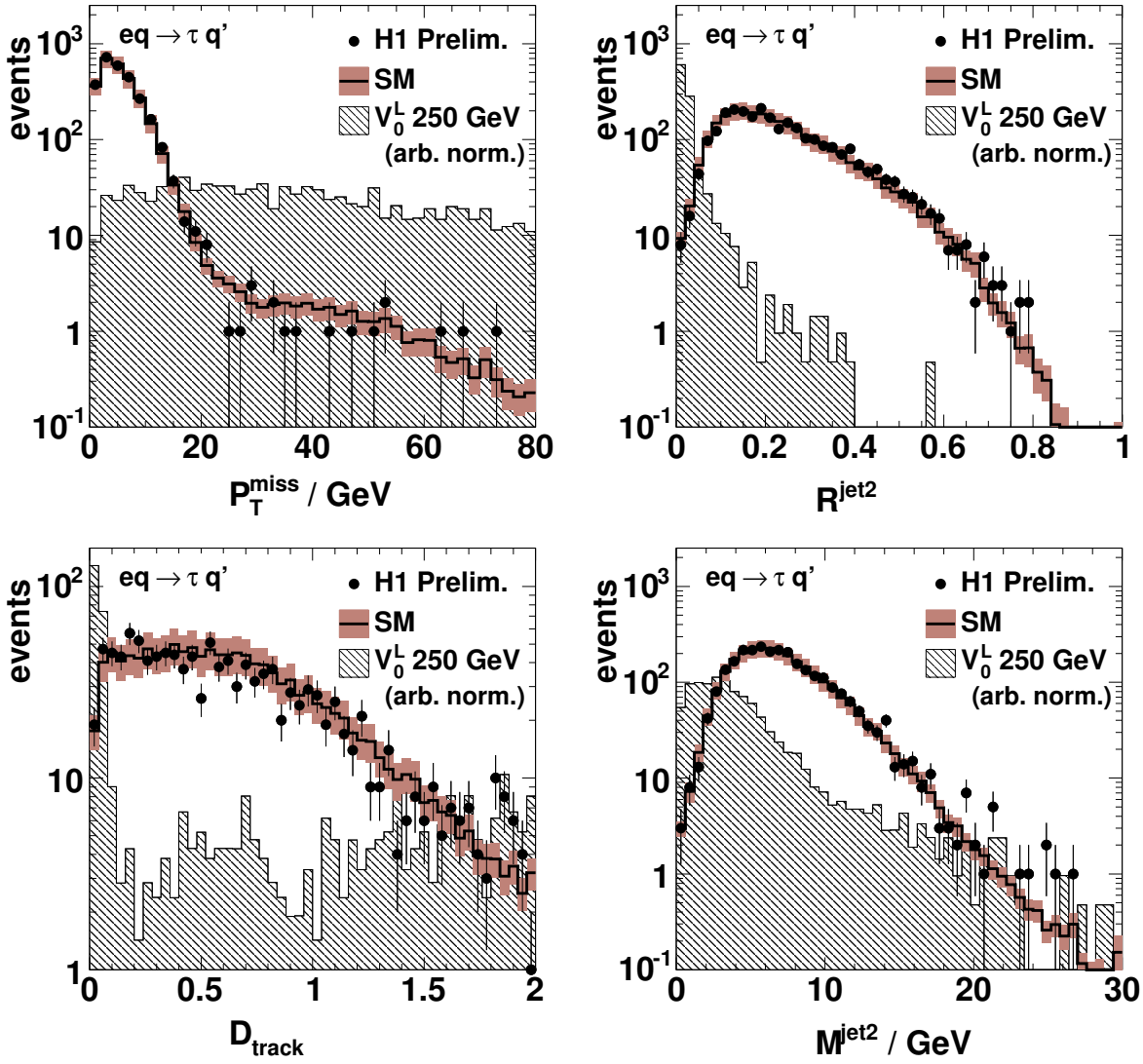

Figure 3: Distributions of H1 data in the tau channel after the first selection step for $\tau + q$ signatures with SM expectation and arbitrarily normalised LFV signal mediated by a vector LQ, V_0^L, of mass 250 GeV decaying to a tau and a quark. Top left: Missing transverse momentum before the cut at 20 GeV to enhance the LFV signal with respect to the SM background. Top right: Radial size of jet2 in the $\eta\phi$-plane with the signal showing the typical very narrow shape of a τ-jet. Bottom left: Distance of the nearest track to the leading track of jet2 showing the difference of isolation between the LFV signal and SM background. Bottom right: Mass of jet2 indicating the low mass of a τ-jet compared to an ordinary hadronic jet.

SM Process	Event generator	MC uncertainty(%)
NC DIS	Rapgap	10
Lepton pair	Grape	10
W-Production	Epvec	15
Photoproduction	Pythia	30

Table 2: Systematic uncertainties for the dominant SM MC used in the analysis.

H1 Preliminary, $\mathcal{L} = 66\ \mathrm{pb}^{-1}$		
	$\mathrm{LQ} \to \mu + q$	$\mathrm{LQ} \to \tau + q$
Data	0	1
Total SM	0.74 ± 0.25	0.56 ± 0.16
NC DIS	0.09 ± 0.05	0.37 ± 0.13
Lepton Pair	0.50 ± 0.24	-
Photoproduction	0.06 ± 0.07	0.13 ± 0.04
W-Production	0.08 ± 0.02	0.06 ± 0.02

Table 3: Numbers of events after the final selection with their total errors. Statistical and systematic errors are added in quadrature.

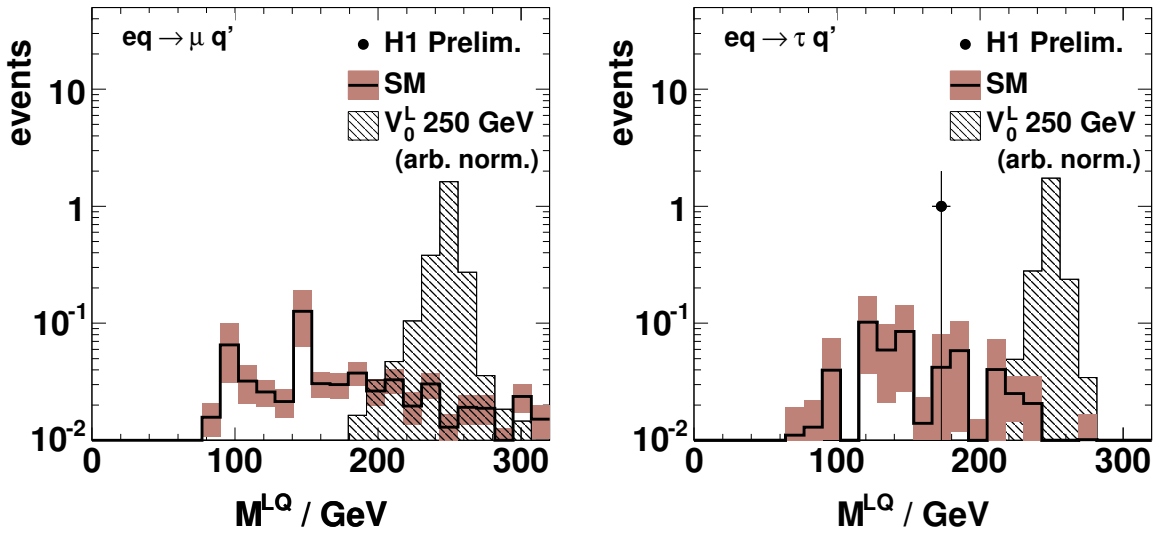

Figure 4: Mass spectra after the final selection for $\mu + q$ signatures (left) and $\tau + q$ signatures (right) compared to a vector LQ, V_0^L, of mass 250 GeV decaying to a muon and a quark (left) or a tau and a quark (right).

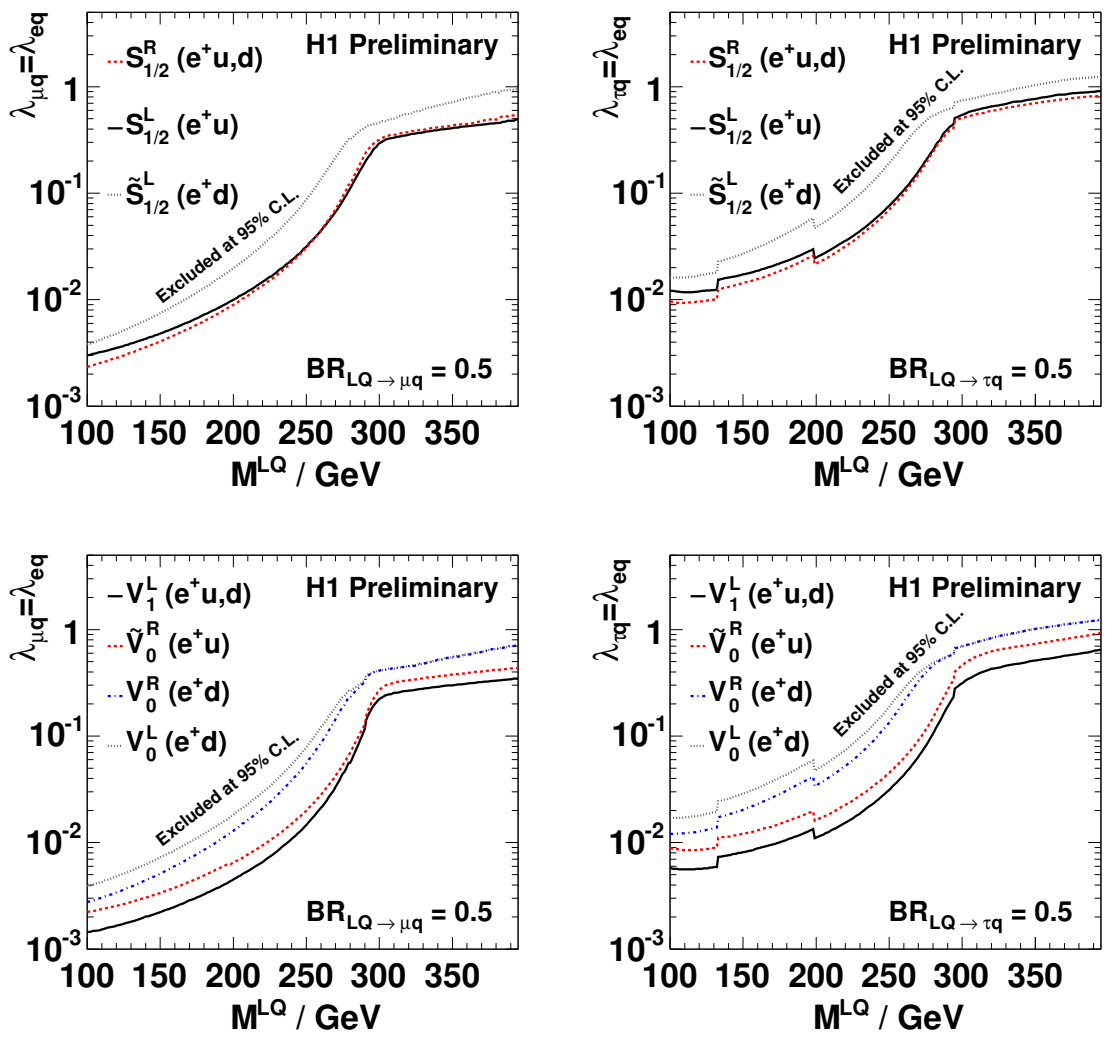

Figure 5: Limits on the coupling constant strength λ_{lq} at 95% C.L. as a function of LQ mass for scalar (top) and vector (bottom) LQs in the muon (left) and tau (right) decay channels.

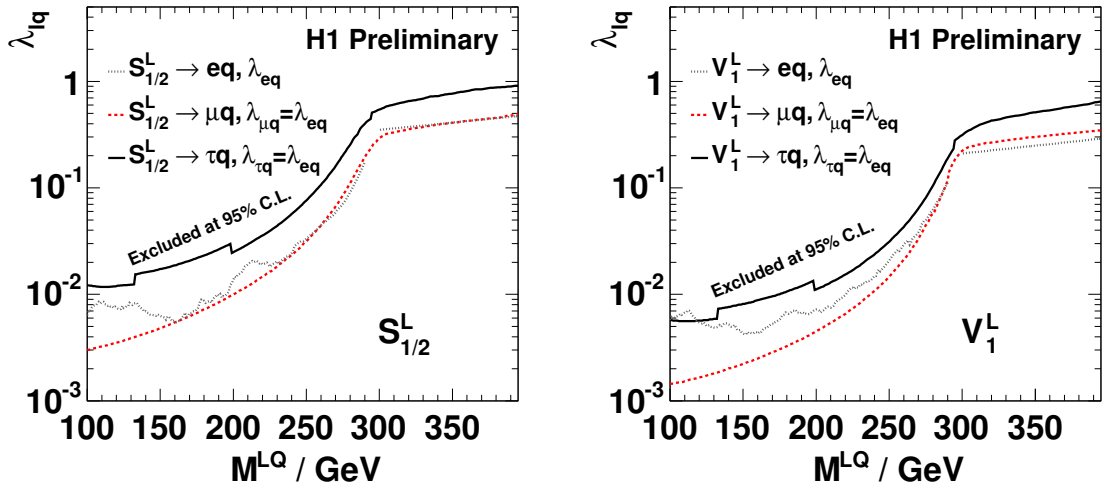

Figure 6: Limit on the coupling strength λ_{lq} at 95% C.L. for $S^L_{1/2}$ and V^L_1 decaying into leptons of the first, second and third generations.

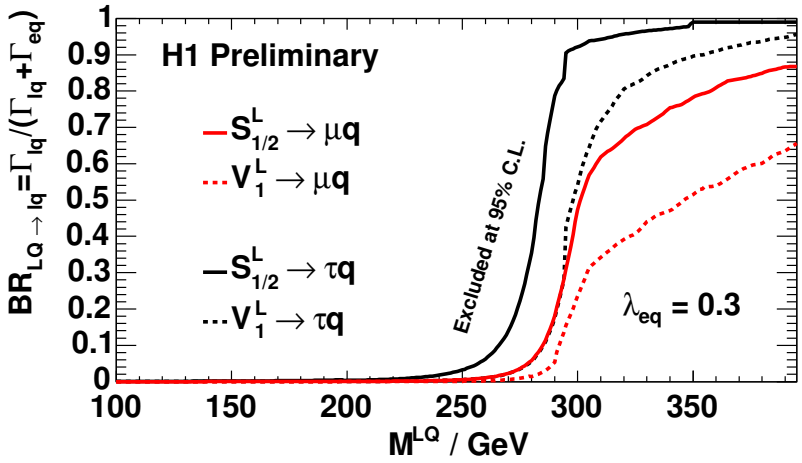

Figure 7: Mass limit of LQs $S^L_{1/2}$ and V^L_1 at 95% C.L. as a function of the branching ratio for $\mathrm{LQ} \to \mu q$ and $\mathrm{LQ} \to \tau q$ with a fixed coupling to first generation leptons at $\lambda_{eq} = 0.3$.